ChemComm

Accepted Manuscript

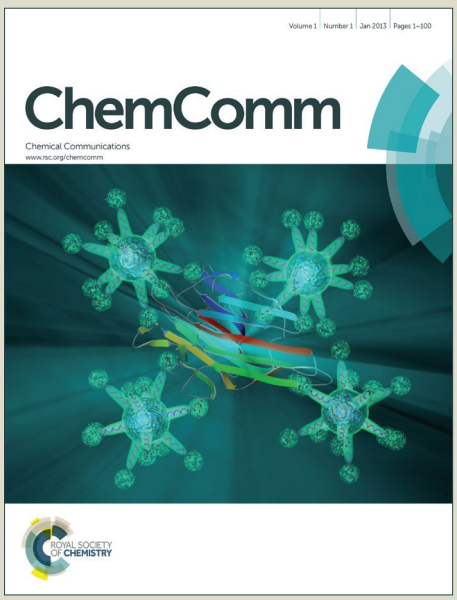

ROYAL SOCIETY OF CHEMISTRY

www.rsc.org/chemcomm

Journal Name

COMMUNICATION

Plasmonic Au nanoparticles embedding enhances the activity and stability of CdS for photocatalytic hydrogen evolution

158440657Received 00th January 20xx,
Accepted 00th January 20xx

DOI: 10.1039/x0xx00000x

www.rsc.org/

Guiyang Yu,[a] Xiang Wang,[b] Jungang Cao,[a] Shujie Wu,[a] Wenfu Yan,[c] and Gang Liu*[a]

The activity and stability of CdS for visible-light-driven hydrogen evolution could be significantly enhanced by embedding plasmonic Au nanoparticles. The plasmon resonance energy field of Au nanoparticles could increase the formation rate and lifetime of e^-/h^+ pairs in CdS semiconductor.

The photocatalytic production of hydrogen using semiconductor is a potential clean process for converting solar energy into chemical fuels. [1] But realizing this process is quite difficult. [2] Up to now, the activity and stability of photocatalyst is far below the requirement of large scale application. [3-5] It is still desirable to introduce novel strategy to design and prepare photocatalysts with high activity and long lifetime.

Plasmonic effect of metal nanostructures has shown significant promise for enhancing the visible light activity of semiconductor photocatalysts.[6] Generally, plasmonic metals are present as nanoparticles dispersed on the surface of semiconductors.[7] Plasmon-excited hot electrons in noble-metal nanoparticles can be transferred to the conduction band of an adjacent semiconductor, and then participate in subsequent chemical reactions.[8] Recently, another plasmonic effect, termed near-field electromagnetic mechanism, was found playing an important role in promoting photocatalytic activity of semiconductors.[9,10] It is derived from the interaction of the semiconductor with electromagnetic fields localized nearby at the plasmonic metal nanostructure. Linic *et al.* reported that these electromagnetic fields are spatially non-homogenous, with the highest intensity at the surface of the metallic nanostructure and decreasing exponentially with distance from the surface within 20-30 nm.[11] Suitable placement of the plasmonic metal and semiconductor should be very important for taking fully advantage of the electromagnetic fields.

Traditionally, plasmonic metal (e.g. Au) is loaded on the surface of semiconductor (Fig 1A). Only small part of semiconductor that closet to the Au nanoparticles could be affected by the electromagnetic fields of plasmonic Au. Core-shell nanostructure geometrically satisfies the full use of spatial electromagnetic fields. It has been demonstrated that a few Au@sulfide core-shell nanostructure could enhance the photocatalytic hydrogen evolution activity. But the efficiencies of these photocatalysts are still low, even under the optimized reaction conditions.

In this work, a strategy that embedding plasmonic Au nanoparticles into CdS semiconductor was attempted (Fig 1B). It possesses the advantage of core-shell nanostructure that could fully use the electromagnetic fields of the Au nanoparticles. The resultant photocatalysts were denoted as x%Au@CdS, where x is the weight percent of Au nanoparticles. The photocatalytic hydrogen evolution activity was improved from 83 $\mu molh^{-1}$ of CdS to 374 $\mu molh^{-1}$ of 0.5%Au@CdS, without the use of any other metal or metal oxide as cocatalysts. The quantum efficiency can reach 12.1 % for 0.5%Au@CdS at 420 nm. When using 0.1wt%Pt as a cocatalyst,

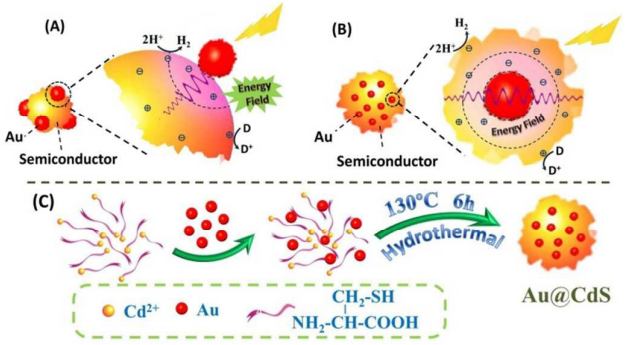

Fig. 1 Illustration of the interaction of the semiconductor with electromagnetic fields localized nearby at the plasmonic Au: (A) Au loaded on the surface of semiconductor (B) Au embedded into the semiconductor. (C) Schematically illustrating the formation of Au@CdS.

[a] *Key Laboratory of Surface and Interface Chemistry of Jilin Province, College of Chemistry, Jilin University, Jiefang Road 2519, Changchun, 130012, China*
[b] *Institute for Integrated Catalysis, Pacific Northwest National Laboratory, Richland, WA 99352, USA*
[c] *A State Key Laboratory of Inorganic Synthesis and Preparative Chemistry, College of Chemistry, Jilin University, Qianjin Road 2699, Changchun, 130012, China .*
†Electronic Supplementary Information (ESI) available: details of the synthesis, characterization, photocatalytic activity measurement, and additional figures. See DOI: 10.1039/x0xx00000x

the quantum efficiency of 0.5%Au@CdS can be further improved to 45.6%. Besides, the photocorrosion drawback of CdS was also overcome by embedding Au nanoparticles. The stability of 0.5%Au@CdS can be maintained more than 100 h, which is much higher than that of CdS.

Au colloid nanoparticles were prepared by a sodium citrate reduction method using $HAuCl_4$ as a precursor.[12, 13] The citrate-protected Au nanoparticles could disperse quite well in the aqueous solution. The diameter of the Au nanoparticles was about 15 nm on average (Fig. 2a). From the HRTEM image (Fig. 2b), an interlayer spacing of 0.24 nm can be observed, which is in good agreement with the *d* spacing of the (111) lattice planes of the *fcc* Au crystal. The synthesis of Au@CdS photocatalysts was accomplished using a cysteine-assisted hydrothermal approach.[12] As shown in Fig. 1C, the synthesis involves two main steps: (1) formation a complex of cysteine-Cd^{2+}, (2) growth of cysteine-Cd^{2+} on the surface of Au nanoparticles. It was followed by the decomposition of cysteine-Cd^{2+} and subsequently forming CdS. The contents of Au in the Au@CdS hybrid nanostructure were controlled by the amount of cysteine-Cd^{2+} in the synthesis process.

The resultant Au@CdS is consisted of uniform small particles (detected by SEM, Fig. S1). Typical transmission electron microscopic (TEM) images of 0.5%Au@CdS and 1%Au@CdS were shown in Fig. 2c-f. The difference in the atomic masses of Au and CdS resulted in relatively clear contrast, which could help us to reveal the nanostructure of Au@CdS.[14] It shows that Au nanoparticles are nearly completely embedded in the CdS bulk structure (Fig. 2c-f). No isolated Au nanoparticles can be observed on the surface of Au@CdS hybrid nanostructure. The position of Au nanoparticles could be clearly distinguished from magnified TEM image of 1%Au@CdS (Fig. 2e). The corresponding electron diffraction pattern exhibits two sets of diffraction patterns, confirming the presence of Au in CdS nanostructures (Fig. 2d inset). An HRTEM image was taken at the edge of 1%Au@CdS (Fig. 2f). The interlayer spacing of 0.34 nm complies with the lattice spacing of the (002) planes of the wurtzite CdS, suggesting that CdS of the composite possesses high degree of crystallinity.

Fig. 3A shows the X-ray diffraction (XRD) patterns of pure CdS and Au@CdS composites with different Au amounts. All

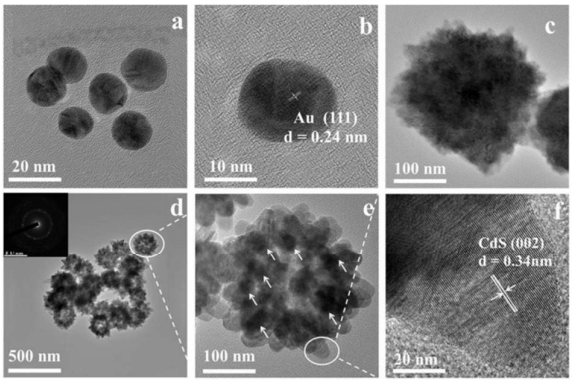

Fig. 2 (a and b) HRTEM images of Au colloid. (c) TEM images of 0.5% Au@CdS. (d and e) TEM and (f) HRTEM images of 1.0%Au@CdS.

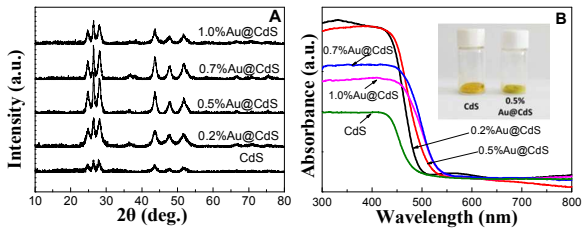

Fig. 3 (A) XRD patterns and (B) UV-vis diffuses reflection spectra of CdS and Au@CdS with different Au contents.

the samples exhibit six main diffraction peaks at 24.8º, 26.5º, 28.2º, 43.7º, 47.8º and 51.8º, which can be ascribed to (100), (002), (101), (110), (103), and (112) planes of hexagonal wurtzite CdS (JCPDS No. 41-1049).[5, 15] The absence of Au diffraction peaks in the patterns of Au@CdS should be due to the low contents of Au. N_2-adsorption results show that the specific surface area of Au@CdS is about 20 m^2g^{-1}, which is a little lower than that of pure CdS (30.1 m^2g^{-1}).

Fig. 3B shows the UV-vis diffuse reflectance spectra of CdS and Au@CdS with different Au contents. CdS exhibits an absorption edge at about 500 nm, corresponding to the bandgap (E_g) of about 2.48 eV. Au@CdS shows a red shift of the absorption edges with the increase of Au contents, which could be ascribed to the presence of Au nanoparticles. The increase of absorption intensity over the visible light region, especially between 500 and 550 nm, should be due to the plasmon resonance feature of Au nanoparticles. Such distinct differences in light absorption can also be observed clearly from the photographs of CdS and Au@CdS (inset Fig. 3B). The surface plasmon absorption of gold nanoparticles (colloid suspension) can be observed maximizing around 520 nm (Fig.S2). This absorption cannot be found in the spectra of Au@CdS. Based on above results, it can be proposed that overlap should exist between plasmon and band-gap absorption.

The photocatalytic H_2 evolution performance of Au@CdS and CdS were evaluated using aqueous solutions containing 0.25 M Na_2SO_3 and 0.35 M Na_2S sacrificial reagent under visible light. Without the use of any other metal or metal oxide as cocatalysts, CdS exhibits an activity of 83 $\mu molh^{-1}$ (Fig. 4A). Under the same reaction condition, Au@CdS exhibit evidently higher catalytic activities. An optimized H_2 evolution activity can be observed over 0.5%Au@CdS, which is about 374 $\mu molh^{-1}$. The apparent quantum efficiency measurement shows that the quantum efficiency of 0.5%Au@CdS is around 12.1% under 420 nm irradiation. The activity could be further improved using additional 0.1wt%Pt as a cocatalyst. Fig. 4B shows that the activity of 0.5%Au@CdS could be improved to 1150 $\mu molh^{-1}$, and the corresponding quantum efficiency is about 45.6% at 420 nm (Fig.4D). This result is much higher than that of many recently reported composite photocatalysts, such as Au/CdS core/shell nanocrystals and the composite of CdS cluster coupled with graphene sheets (loading 0.5 wt% Pt as a cocatalyst, Table S1).[16]

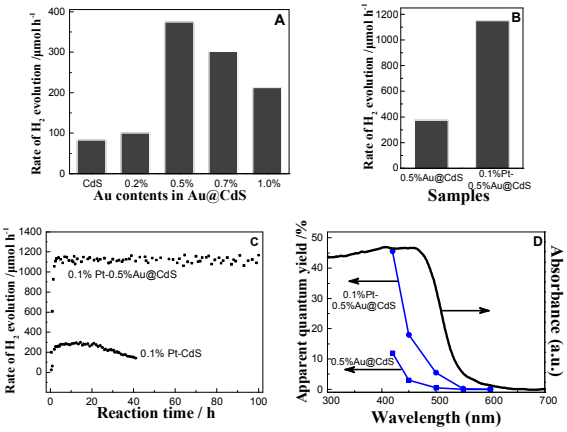

Fig. 4 Photocatalytic H_2 evolution activity of (A) pure CdS and Au@CdS with different Au contents (B) 0.5%Au@CdS and 0.1%Pt-0.5%Au@CdS under visible light irradiation. (C) Typical time course for H_2 production over 0.1%Pt-0.5%Au@CdS and 0.1%Pt-CdS under visible light irradiation. Reaction condition: 0.1 g photocatalysts in 100 mL Na_2S (0.35 M)-Na_2SO_3 (0.25 M) solution, 300 W Xe-lamp equipped with cut-off filter ($\lambda \geq 420$ nm). (D) Influence of wavelength on the apparent quantum yield for hydrogen evolution. Reaction condition: 0.1 g 0.5%Au@CdS and 0.1%Pt-0.5%Au@CdS in Na_2S (0.35 M) and Na_2SO_3 (0.25 M) aqueous solution under various wavelengths of 420, 450, 500, 550, and 600 nm.

More importantly, the high catalytic activity could be well maintained without notable decrease during the entire reaction time investigated (Fig.4C). The cumulated reaction-time is more than 100 h. Under the same reaction condition, obvious decrease of activity can be observed over CdS photocatalyst (Fig.4C). This result suggests that embedding Au nanoparticles could also promote the stability of CdS. X-ray photoelectron spectroscopy (XPS) was carried out to detect the chemical state of Cd in the samples of fresh CdS, 0.5%Au@CdS and used 0.5%Au@CdS after 100 h test (Fig. S3). No obvious changes for the peak of Cd $3d_{5/2}$ at 404.6 eV can be observed among above three samples. It confirms that the chemical state of Cd has no change before and after long-time reaction test.

The above observations show that the presence of Au nanoparticles in the hybrid nanostructures effectively enhance the photocatalytic activity and stability toward visible-light-driven hydrogen evolution. Two main mechanisms have ever been proposed to explain the rate enhancement by plasmonic Au nanoparticles. One is plasmon-excited charges injection from Au to the semiconductors, the other is radiative energy transfer from plasmonic Au to the semiconductor. In the former process, the Au nanoparticles absorb light and transfer the energetic electron (formed in the surface plasmon resonance) to the nearby semiconductor. So the maximum contribution of Au nanoparticles to the photocatalytic activity should occur at the strongest plasmon resonance absorption. In this case, the photocatalytic activity of 0.5%Au@CdS is very low at 500 nm (10.7 $\mu molh^{-1}$) and 550 nm (0.5 $\mu molh^{-1}$), suggesting that energetic electrons generated from plasmons in Au nanoparticles are not the main contributor to the enhancement of hydrogen evolution. Besides, it should be noted that the Au nanoparticles were coated with non-

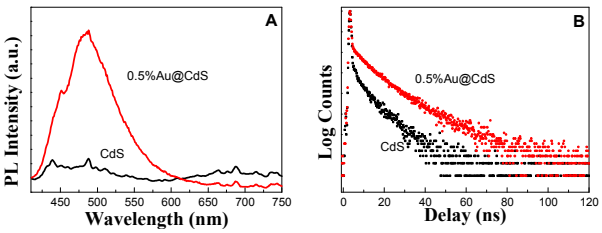

Fig. 5 (A) Photoluminescence spectra of CdS and 0.5%Au@CdS. The excitation wavelength is 390 nm. (B) Photoluminescence decays of CdS and 0.5%Au@CdS.

conducting organic stabilizer molecules. These stabilizer molecules could separate the metal and semiconductor layers, and limit the electron transfer between the semiconductor and the metal.[17] Therefore, the enhancement of the photocatalytic activity and stability is most likely associated with plasmon resonance energy transfer. Plasmon excitation of Au by absorption of a photon results in a plasmon resonance energy field, which could positively influence excitation of CdS and result in an increased formation rate of e^-/h^+ in CdS.

For supporting experimental evidence to understand the promotion effects of Au nanoparticles, the photoluminescence (PL) spectra of CdS and 0.5%Au@CdS were taken (Fig. 5A). The PL signal at 480 nm can be assigned to the band-edge emission of CdS.[18, 19] Compared with pure CdS, this signal in the spectrum of 0.5%Au@CdS was dramatically enhanced by about 7.4 times. It is known that semiconductor emission is proportional to the concentration of electron-hole pairs in the semiconductor. This enhancement should directly reflect the increased rate of e^-/h^+ formation in the CdS part of 0.5%Au@CdS. It is tightly related to the surface plasmon resonance of Au nanoparticles. Due to the surface plasmon of the Au nanoparticles matches the band-gap adsorption of the CdS, the resulting resonance can lead to an effective energy transfer from the metal surface to CdS, which induced an enhancement of the e^-/h^+ formation. Time-resolved PL measurements were also carried out, which can reflect the lifetime of photoexcited electrons in a certain degree.[19, 20] Fig. 5B shows that the intensity of 0.5%Au@CdS decays much slower than that of the bare CdS, indicating that 0.5%Au@CdS have a longer luminescence lifetime than that of CdS. The observed decay reflect the lifetime of photoexcited electrons and its transients, which is in agreement with our interpretation of activity. That is the presence of Au nanoparticles endows the photoexcited electrons in CdS semiconductor with much longer lifetime to reduce H^+ forming H_2. And the corresponding holes are with enough time to oxidize the sacrificial agents. It should be mentioned that the PL spectra of Au@CdS is a little difference from that of other noble metal loading photocatalyst system. The PL spectra usually be quenched after loading Au or Pt nanoparticles, due to these metals act as cocatalysts trapping photoexcited electrons. In our case, the increase of the PL spectrum of Au@CdS should be ascribed to the energy transfer from Au to CdS. The presence of non-conducting molecules on the

surface of Au nanoparticles limits the electron transfer between the semiconductor and the metal.

The influence of the position of Au nanoparticles on the photocatalytic H_2 evolution activity was also investigated. In a separated experiment, the activity of Au nanoparticles attaching on the CdS surface was detected (Fig. S4). This composite could enhance the photocatalytic hydrogen production in a certain degree compared with pure CdS, but its activity is much lower than that of 0.5%Au@CdS. Based on these results, we summarize the reaction mechanism. Plasmon excitation of Au nanoparticles results in an energy field, which positively influences CdS excitation forming e^-/h^+ pairs. The plasmon-induced electron-hole pair formation is the highest in the parts of the CdS closet to the Au nanoparticles. Embedding Au nanoparticles into CdS could take fully advantage of electromagnetic fields at the surface of the Au nanoparticles to improve the formation of e^-/h^+ pairs, and then increase the activity of photocatalysts.

In summary, plasmonic Au nanoparticle with an average diameter of 15 nm has been successfully embedded into CdS with a cysteine-assisted hydrothermal approach. The photocatalytic hydrogen evolution activity and stability of the composite Au@CdS could be significantly improved comparing with that of pure CdS. PL characterization shows that both the formation rate and lifetime of photoexcited e^-/h^+ were dramatically increased when Au nanoparticles were embedded into CdS, which should be responsible for the high activity of Au@CdS. All these enhancements can be attributed to the effective energy transfer from the Au surface to CdS. This embedding nanostructure could take fully advantage of electromagnetic fields at the surface of the Au nanoparticles under visible light illumination.

The authors acknowledge supports from the National Natural Science Foundation of China (21473073), the Development Project of Science and Technology of Jilin Province (20130101014JC), and the Open Project of State Key Laboratory of Inorganic Synthesis and Preparative Chemistry. Dr Xiang Wang gratefully acknowledges the US Department of Energy (DOE), Office of Science, Office of Basic Energy Sciences, Chemical Sciences, Geosciences, and Biosciences Division for the support of this work.

Notes and references

1 (a) A. Kudo and Y. Miseki, *Chem. Soc. Rev.*, 2009, **38**, 253; (b) X. Chen, S. Shen, L. Guo, and S. S. Mao, *Chem. Rev.*, 2010, **110**, 6503;(c) J. Kim and W. Choi, *Energy & Environ. Sci.*, 2010, **3**, 1042; (d) K. Maeda, K. Teramura, D. Lu, T. Takata, N. Saito, Y. Inoue and K. Domen, *Nature*, 2006, **440**, 295.

2 (a) X. Wang, Q. Xu, M. Li, S. Shen, X. Wang, Y. Wang, Z. Feng, J. Shi, H. Han and C. Li, *Angew. Chem. Int. Ed.*, 2012, **51**, 13089; (b) G. Liu, X. Wang, X. Wang, H. Han and C. Li, *J. Catal.*, 2012, **293**, 61; (c) J. Li, S. K. Cushing, P. Zheng, T. Senty, F. Meng, A. D. Bristow, A. Manivannan and N. Wu, *J. Am. Chem. Soc.*, 2014, **136**, 8438.

3 (a) X. Wang, G. Liu, L. Wang, Z.-G. Chen, G. Q. M. Lu and H.-M. Cheng, *Adv. Energy Mater.*, 2012, **2**, 42; (b) D. Wang, T. Hisatomi, T. Takata, C. Pan, M. Katayama, J. Kubota and K. Domen, *Angew. Chem. Int. Ed.*, 2013, **52**, 11252; (c) G. Yu, L. Geng, S. Wu, W. Yan and G. Liu, *Chem. Comm.,* 2015, **51**, 10676; (d) G. Liu, J. Han, X. Zhou, L. Huang, F. Zhang, X. Wang, C. Ding, X. Zheng, H. Han and C. Li, *J. Catal.*, 2013, **307**, 148; (e) X. Wang, S. Shen, S. Jin, J. Yang, M. Li, X. Wang, H. Han and C. Li, *Phys. Chem. Chem. Phys.*, 2013, **15**, 19380.

4 (a) N. Bao, L. Shen, T. Takata and K. Domen, *Chem. Mater.*, 2008, **20**, 110; (b) L. Huang, X. L. Wang, J. H. Yang, G. Liu, J. F. Han, and C. Li, *J. Phys. Chem. C* 2013, **117,** 11584.

5 J. Jin, J. Yu, G. Liu and P. K. Wong, *J. Mater. Chem. A*, 2013, **1**, 10927.

6 (a) S. Sun, H. Liu, L. Wu, C. E. Png and P. Bai, *ACS Catal*., 2014, **4**, 4269; (b) Y. Zhong, K. Ueno, Y. Mori, X. Shi, T. Oshikiri, K. Murakoshi, H. Inoue and H. Misawa, *Angew. Chem. Int. Ed.*, 2014, **53**, 10350; (c) N. Kumar, V. K. Komarala and V. Dutta, Chem. Eng. J., 2014, 236, 66; (d) E. Khon, A. Mereshchenko, A. N. Tarnovsky, K. Acharya, A. Klinkova, N. N. Hewa-Kasakarage, I. Nemitz and M. Zamkov, Nano Lett, 2011, 11, 1792.

7 (a) S. Eustis and M. A. el-Sayed, *Chem. Soc. Rev.*, 2006, **35**, 209; (b) X. Zhang, Y. Liu, S.-T. Lee, S. Yang and Z. Kang, *Energy & Environ. Sci.*, 2014, **7**, 1409. (c) X. Yu, A. Shavel, X. An, Z. Luo, M. Ibanez and A. Cabot, *J. Am. Chem. Soc.*, 2014, **136**, 9236; (d) A. Tanaka, K. Fuku, T. Nishi, K. Hashimoto and H. Kominami, *J. Phys. Chem. C*, 2013, **117**, 16983; (e) M. Murdoch, G. I. Waterhouse, M. A. Nadeem, J. B. Metson, M. A. Keane, R. F. Howe, J. Llorca and H. Idriss, *Nat. Chem.*, 2011, **3**, 489.

8 (a) S. Linic, P. Christopher, H. Xin and A. Marimuthu, *Acc. Chem. Res.*, 2013, **46**, 1890; (b) D. B. Ingram, P. Christopher, J. L. Bauer and S. Linic, *ACS Catal.*, 2011, **1**, 1441; (c) J. Long, H. Chang, Q. Gu, J. Xu, L. Fan, S. Wang, Y. Zhou, W. Wei, L. Huang, X. Wang, P. Liu and W. Huang, *Energy & Environ. Sci.*, 2014, **7**, 973.

9 Z. W. Seh, S. Liu, M. Low, S. Y. Zhang, Z. Liu, A. Mlayah and M. Y. Han, *Adv. Mater.*, 2012, **24**, 2310.

10 R. Amrollahi, M. S. Hamdy and G. Mul, *J. Catal.*, 2014, **319**, 194.

11 S. Linic, P. Christopher and D. B. Ingram, *Nat Mater*, 2011, **10**, 911.

12 (a) W. T. Chen, Y. K. Lin, T. T. Yang, Y. C. Pu and Y. J. Hsu, *Chem. Comm.*, 2013, **49**, 8486; (b) X. Ji, X. Song, J. Li, Y. Bai, W. Yang and X. Peng, *J. Am. Chem. Soc.*, 2007, **129**, 13939.

13 W.-T. Chen, T.-T. Yang and Y.-J. Hsu, *Chem. Mater.*, 2008, **20**, 7204.

14 E. Ha, L. Y. Lee, J. Wang, F. Li, K. Y. Wong and S. C. Tsang, *Adv. Mater.*, 2014, **26**, 3496.

15 (a) Y. Hu, X. Gao, L. Yu, Y. Wang, J. Ning, S. Xu and X. W. Lou, *Angew. Chem. Int. Ed.*, 2013, **52**, 5636; (b) Z. Ren, J. Zhang, F.-X. Xiao and G. Xiao, *J. Mater. Chem. A*, 2014, **2**, 5330.

16 (a) Q. Zhao, M. Ji, H. Qian, B. Dai, L. Weng, J. Gui, J. Zhang, M. Ouyang and H. Zhu, *Adv. Mater.*, 2014, **26**, 1387; (b) Q. Li, B. Guo, J. Yu, J. Ran, B. Zhang, H. Yan and J. R. Gong, *J. Am. Chem. Soc.*, 2011, **133**, 10878; (c) X. Ma, K. Zhao, H. Tang, Y. Chen, C. Lu, W. Liu, Y. Gao, H. Zhao and Z. Tang, *Small*, 2014, **10**, 4664.

17 D. B. Ingram and S. Linic, *J. Am. Chem. Soc.*, 2011, **133**, 5202.

18 (a) A. E. Saunders, I. Popov and U. Banin, *J. Phys. Chem. B*, 2006, **110**, 25421; (b) M. Li, X.-F. Yu, S. Liang, X.-N. Peng, Z.-J. Yang, Y.-L. Wang, and Q.-Q. Wang, *Adv. Funct. Mater.* 2011, **21**, 1788.

19 P. Guo, J. Xu, X. Zhuang, W. Hu, X. Zhu, H. Zhou, L. Tang and A. Pan, *J. Mater. Chem. C*, 2013, **1**, 566.

20 (a) T.-T. Yang, W.-T. Chen, Y.-J. Hsu, K.-H. Wei, T.-Y. Lin and T.-W. Lin, *J. Phys. Chem. C*, 2010, **114**, 11414; (b) T. Simon, N. Bouchonville, M. J. Berr, A. Vaneski, A. Adrović, D. Volbers, R. Wyrwich, M. Döblinger, A. S. Susha, A. L. Rogach, F. Jäckel, J. K. Stolarczyk, and J. Feldmann, *Nat. Mater.*, 2014, **13**, 1013.

